Eur. Phys. J. E (2017) **40**: 45
DOI 10.1140/epje/i2017-11534-4

THE EUROPEAN PHYSICAL JOURNAL E

Regular Article

# Exploring the physics of sand drawings: The role of craters, furrows and piles

Jorge González-Gutiérrez and J.C. Ruiz-Suárez[a]

CINVESTAV-Monterrey, PIIT, Nuevo León, 66600, Mexico

Received 28 October 2016 and Received in final form 3 March 2017
Published online: 12 April 2017 – © EDP Sciences / Società Italiana di Fisica / Springer-Verlag 2017

**Abstract.** Few years ago an article addressing the physics behind abstract paintings was published by Herczyński *et al.* (Phys. Today **64**, 31 (2011) issue No. 6). The authors aimed to understand how artists like Jackson Pollock manipulated paints to create pieces of art where the theory of fluid dynamics had a clear and perceivable role. Scaling laws were found to explain the plasticity observed in the artists's traces that we admire in worldwide museums. Because sand drawings are not only wonderful artistic expressions but also intangible cultural heritages of humanity, we wonder if they could be analyzed in a similar fashion. Our goal is to explore the physics behind the formation of such drawings. In order to do so, we carry out experimental studies on the formation of sand cavities, furrows and piles, which individually or interconnected, give rise to artistic patterns. Moreover, in order to manipulate such three observables, some control parameters are needed. Altogether, they conform into simple exponential and power laws that collapse when a scaling is performed.

## 1 Introduction

The physical properties of fluids are key elements behind the artistic works of painters. Examples are many. During an experimental painting workshop held in New York in 1936, David Alfaro Siqueiros, a recognized Mexican muralist, developed what he called *accidental painting*. The technique consisted in pouring, on a horizontal surface, two or more layers of paint of different density and color to create fine inhomogeneous textures [1]. The Rayleigh-Taylor instability [2,3] was Siqueiros's assistant: the less dense fluid emerges from the bottom of the paint layer to form beautiful stains [4,5]. Sam Francis, an artist influenced by abstract expressionism, developed a style where discrete drop splashes or spray points dominate the canvases [6–10]. Robert Motherwell took advantage of the properties of fluids and the geometry of the jets to create a cascade of drops capable of creating dazzling paintings [6, 11]. The artwork of Jackson Pollock is a clear example where many of the properties of the fluids are involved in creating, by pouring and dripping liquids on horizontal canvas, stunning paintings. In the words of Herczyński *et al.*: "Pollock creatively gave some responsibility for the appearance of his work to natural phenomena, inviting fluid dynamics as a co-author" [6].

Has any other theory in physics a similar co-authorship in artistic creations where fluid-like materials are used? The answer to this question requires not only a careful analysis of the creation process but also experimental studies of the emerging phenomena that appear when complex fluids (granular media, foams or emulsions) are manipulated. In the last several years sand has been used to create vivid stories [12] or mega-drawings in open spaces [13] (see fig. 1(a)–(c) and fig. 2(a), (b), respectively). In the archipelago of Vanuatu, graceful and symmetrical geometric patterns on sand have been historically developed as a form of communication among members with more than eighty different languages [14–16] (see fig. 2(c)). Sona drawings of the Chokwe people of Angola and Zaire are a particularly attractive form of mirror curves [15,17,18] and Kolam patterns are considered traditional objects for decorating courtyards, temples and prayer rooms in South India [15,19,20].

At first glance it seems that such granular drawings bear a great complexity; however, if one looks carefully, simple forms nest in them. Sand drawings are made either by making cavities and furrows with bars or fingers, or by a gentle deposition of piles. If the desire of the artist is to create a single geometrical motif, only one of these techniques is sufficient (see fig. 2); but if a high complexity is required, the artist must interconnect the three of them (see fig. 1(d)).

In analogy with penetrometer tests in standard soil mechanics, several groups have investigated the immersion and displacement of objects as a way to reveal the rheology of dense granular materials [21–24]. In general, in a quasistatic regime, the shape and size of the penetrating objects, size of grains, and packing fraction, are parameters

[a] e-mail: jcrs.mty@gmail.com

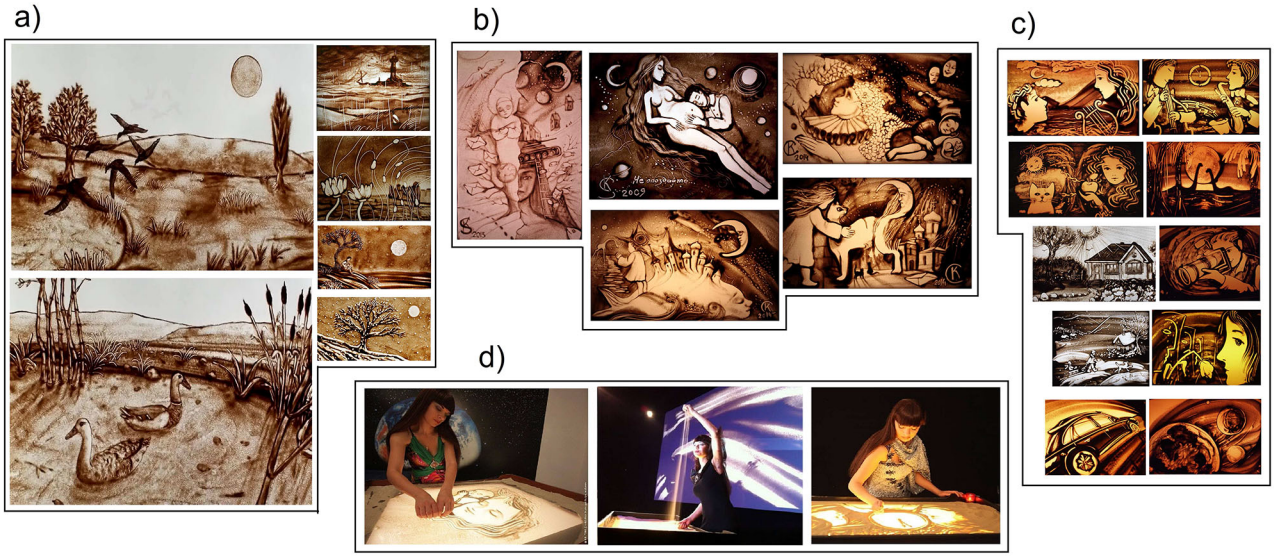


**Fig. 1.** (a) Drawings by D. Myriam. (b) Drawings by K. Simonova. (c) Drawings by A. Woinowa. (d) Artist (K. Simonova) drawing a motive on sand.

**Fig. 2.** (a) Mega drawings by Jim Denevan. (b) Mega drawings by Andres Amador. (c) Artist of Vanuatu preparing a drawing on sand and three drawings by artists of Vanuatu.

that influence the short-range nature of frictional interactions. These, along with long-range forces (chains that are formed and cut) determine the rheology of the granular systems. On the other hand, different mechanisms of deposition such as pouring rate, height and deposition of jet size, which induce the formation of sandpiles [25–27], are strongly affected by some of the above parameters.

While many studies can be associated to precursory phenomena that generate the formation of craters, furrows or piles [28–34], there is no available information on how these observables scale with the control parameters manipulated by artists to create artificial complex drawings.

With the aim to understand how artists manipulate sand to create pieces of art where the theory of granular media has a clear and perceivable role, we carried out experiments of penetration, displacement, and sand deposition. We found that exponential and power laws describe how the size grows for cavities, furrows, and piles.

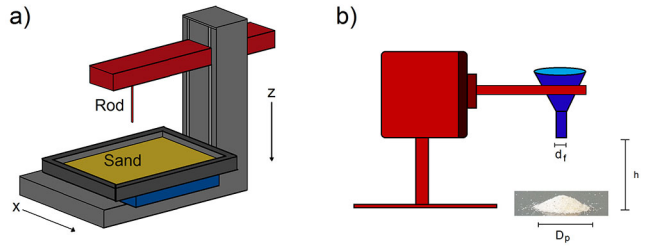


**Fig. 3.** Experimental set-up. (a) A schematic diagram of the experimental apparatus to form cavities and furrows. The bar attached to the machine penetrates sand at depth $z$. To form furrows the bar is displaced in $x$. (b) Set-up used for depositing a certain mass of grains.

## 2 Experimental details and results

Firstly, we used rigid cylindrical bars of three diameters $d = 0.7, 1.1$ and $1.8\,\mathrm{cm}$ to form cavities and furrows by penetrating and sliding into sand contained in a square box $40\,\mathrm{cm}$ per side and $6\,\mathrm{cm}$ of height, filled with polydisperse millimetric glass beads (diameter $0.2\,\mu\mathrm{m} < D_g < 1\,\mathrm{mm}$ and density $\rho = 2.2\,\mathrm{g\,cm^{-3}}$), see fig. 3(a). These diameters cover the size of the distal phalanges of the index, middle, ring and pinky fingers of artists, as well as the spikes of the rakes used by them. The speed of the rods we used in the experiments reported here was $v = 0.005\,\mathrm{m/s}$. Secondly, we used smalls funnels of different diameter to deposit sand (diameter $13.1\,\mu\mathrm{m} < D_g < 0.806\,\mathrm{mm}$ and density $\rho = 2.5\,\mathrm{g\,cm^{-3}}$) on a flat surface, see fig. 3(b). The granular medium was prepared by stirring the grains, then the surface was flattened using a rod. The volume fraction was $\phi = 0.9$ and 0.91, respectively. The sand deposition experiment consists in the deposition of grains discharged onto a smooth surface, see fig. 3(b). A small funnel with an orifice of diameters $d_f = 2.6, 3.2$ and $3.6\,\mathrm{mm}$ is placed at a height $h = 10$–$60\,\mathrm{mm}$ by a mechanical arm. The pictures were taken with a digital camera Pixelink PL - B742V.

The formation of cavities left by introducing bars of various diameters into sand, are exemplified in fig. 4(a). We measured the diameters $D$ of such cavities to see how they correlate against the penetration $z$. In fig. 4(b) we plot the scaled data $D/d$ *vs.* $z/d$ and clearly observe that they collapse and grow exponentially. The exponential growth is fitted by the following function:

$$D/d = \delta\left(1 - e^{-(z/d-\epsilon_1)\psi_1}\right), \qquad (1)$$

where $\delta$ is the saturation value $2.95 \pm 0.027$, $\epsilon_1 = -0.37 \pm 0.029$ and $\psi_1 = 1.2 \pm 0.071$. Note that there is a penetration where the diameter of the cavities saturates. This tells us that the volume occupied by the bar inside the sand is not equal to the volume of the crater, probably due to expansion of the material during the penetration of the bar.

Next, we analyze furrows made by rods buried in sand that are moved horizontally, see fig. 5(a). A bar that moves through a granular medium produces a bifurcation behavior depending on the initial packing fraction. The result is

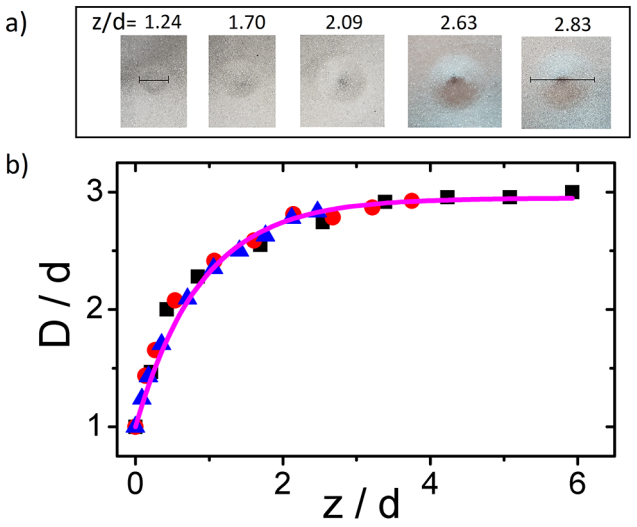


**Fig. 4.** The formation of cavities. (a) A sequence of cavities generated by using a penetration bar method at $z/d = 1.24$–$2.28$. (b) The size of cavities $D/d$ as a function of $z/d$ for rods of diameter $d = 0.7, 1.1$ and $1.8\,\mathrm{cm}$ (squares, circles and triangles, respectively). The magenta line is the best fit, see text.

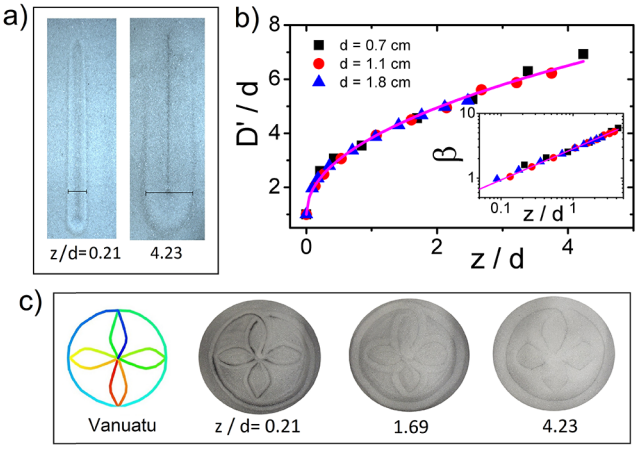


**Fig. 5.** The formation of furrows. Furrows generated by a bar at $z/d = 0.21$ and 4.23 (a). The external width of the furrows $D'$ as a function of $z$ for rods with axial spherical geometry of diameter $d = 0.7, 1.1$ and $1.8\,\mathrm{cm}$ (circles, diamonds and triangles, respectively) (b). Inset: $\beta$ (the first term in eq. (2)) as a function of $z/d$ for rods of diameter $d = 0.7, 1.1$ and $1.8\,\mathrm{cm}$. The magenta line is the best fit for both. (c) The evolution of a Vanuatu-like pattern as a function of $z/d$. Clearly, blurring increases with $z/d$.

that, above a critical packing fraction, the drag force oscillates [35]. Below, it has a complex dynamics. According to the packing fraction in our system, we carried out experiments in the oscillatory regime. The larger the diameter of the rod $d$, the wider the furrow $D'$. $D'/d$ as a function of $z/d$ follows a power law, see fig. 5(b). It is easy to show that the data are fitted using the following equation:

$$D'/d = (a_f/d)(z/d)^{b_f} + 1, \qquad (2)$$

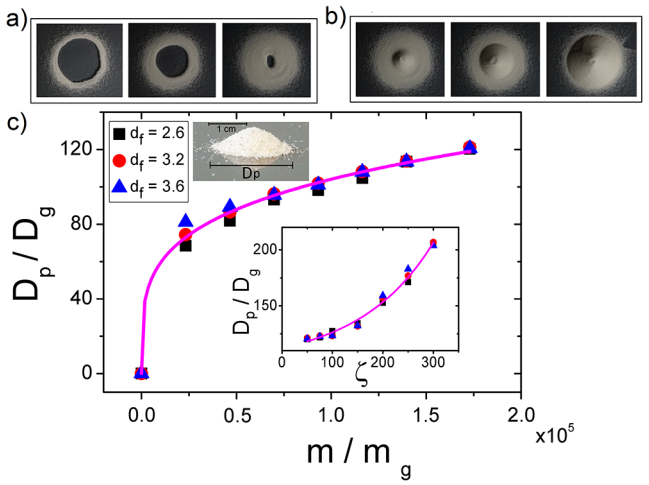


**Fig. 6.** Sand deposition. (a) First growth stage of sand piles. The distribution of grains is obtained on the surface with a low friction. (b) The distribution of grains occurs on top of the layer of grains already deposited in a high friction regime (second stage). (c) $D_p/D_g$ *vs.* $m/m_g$ at funnel diameters $d_f = 2.6, 3.2$ and 3.6 mm, and $h = 10$ mm. Note that for small masses $D_p$ values have more dispersion. See text for an explanation. Inset: the upper image in the inset shows the distribution of grains after being released at $d_f = 2.6$ mm and $h = 10$ mm. The plot in the inset is $D_p/D_g$ *vs.* $\zeta$ for the same funnel diameter.

where $a_f = 2.83 \pm 0.14$ and $b_f = 0.48 \pm 0.03$. The relevance of this result is that to perform a design of a drawing at high penetration depths, it is necessary to increase the area where the drawing is made. On the contrary, a blurred aspect of the drawing appears because the furrows overlap as a result of their growth with the depth of penetration, see the Vanuatu-like drawing for different penetrations in fig. 5(c). Clearly, shallow penetrations are preferred for well-defined drawings.

Since sand deposition is one of the main maneuvers (for at least three of the above artists) in granular drawing, we carry out a sand deposition experiment on a flat and smooth surface using a small funnel. We observe two distinctive growth stages as a function of mass $m$ (as a measure of the number of grains in the funnel), see fig. 6. For small $m$ (first stage) the complete distribution of the grains is obtained on the surface with a low friction, see fig. 6(a). The area occupied by these grains depends strongly on the diameter of the funnel. However, when the mass increases (second stage) the distribution of grains occurs on top of the layer of grains already deposited (high friction), see fig. 6(b).

We found that the diameters of the piles in terms of the mean diameter of the size distribution of the sand $D_p/D_g$ grow as a power law as a function of $m/m_g$, see fig. 6(c). Here, $m_g$ is the average mass of the grains. The solid line is the best fit using the following expression:

$$D_p/D_g = a_p(m/m_g)^{b_p}, \tag{3}$$

where $a_p$ and $b_p$ are $6.29 \pm 0.081$, and $0.24 \pm 0.001$, respectively. In the inset of fig. 6(c) we plot $D_p/D_g$ as a function of the relative height $\zeta$, where $\zeta = h/D_g$ ($h$ being the distance from the funnel aperture to the surface). The solid line is the best fit using the following expression: $D_p/D_g = a' + b'e^{c'\zeta}$, where $a'$, $b'$ and $c'$ are $98.49 \pm 9.81$, $-14.11 \pm 1.57$ and $-0.0068 \pm 0.001$, respectively. The above equations tell us that, to perform a design of a drawing using large piles, it is necessary to increase the sand mass or the relative height. In addition, a blurred aspect of the drawing could appear when the piles overlap as a result of their growth, as the Vanuatu-like drawing in fig. 5(c). Therefore, to make well-defined drawings, a small mass of sand or low relative height $\zeta$ are preferred.

## 3 Discussion

In the Vanuatu archipelago, a unique and complex tradition of sand drawing has been preserved [14–16]. This *writing* is an artistic expression employed in contemplative, communication and rituals contexts. The drawings are produced directly on the ground, in sand, volcanic ash or clay. An artist must use a finger to trace craters and continuous furrows on an imaginary grid that allows him to produce a graceful composition of geometric patterns, see fig. 2(c). In fact, in a similar fashion, the elaboration of complex sand drawings in Africa begins when an artist uses the index and ring fingers of his/her right hand to mark the craters in a rectangular array. Afterwards, the storyteller draws furrows, usually with the index finger of his/her right hand [15,17,18].

Note that in the drawings shown in fig. 2(c), the furrows are not blurred despite being intertwined. Our results suggest that the reason is that they have a perfect balance between design and dimensions. If a drawing is made on the same rectangular grid at high penetration depths, cavities and furrows could overlap and generate a blurred appearance, as we can see in fig. 5(c). This means that shallow penetrations are convenient to elaborate well-defined drawings in a small rectangular array. In contrast, at higher penetration depths such balance is achieved only in larger rectangular boxes.

Equations (1) and (2) teach us that cavities grow exponentially with $z$, while furrows grow as a power law. This could be used to understand how the drawings can be scaled: the size of cavities saturate and furrows continuously grow. Thus, artists must not only use bars of larger diameter but also change the relationship between the penetration depths among cavities and furrows to made the correct shapes of the original design. Moreover, if a design has sand piles, the artist must increment the sand mass or relative height $\zeta$ according to eq. (3).

Mega structures on a sand beach are drawings made by a set of lines of more than one meter width, covering areas greater than 200 square meters, as we can see in fig. 2(a), (b). One could think that if artists want to form such wide furrows, they must use deep penetration with a large flat paddle. Of course, this is a significant loss of resources for the artist. Fortunately, there is an elegant solution. Jim Denevan and Andres Amador use a rake to

remove sand and form small parallel furrows, altogether forming a continuous brushstroke on the beach [13], see fig. 2(a). The rake is dragged on a large sandy surface to create sumptuous motifs, see fig. 2(a), (b). It is evident, by observing such drawings, that these aesthetic figures are obtained with much less energy by the use of slight penetration made by a rake with a large number of spikes to form adjacent furrows [28–32].

To avoid the blurred appearance in mega drawings, it is necessary the use of the correct separation between the rake teeth. According to eq. (2) we could make a prediction: if the weight of the rake and compaction of sand allow the teeth to reach a penetration depth $z = 2d$, it is clear that the minimum separation among the teeth, must be greater than five times $d$.

Other modern artists also use furrows, craters, and sandpiles to generate beautiful sand drawings on a flat surface [12]. Figure 1(d) shows an artist drawing a picture in this fashion and fig. 1(a)–(c) shows some final beautiful drawings. One of the functions of the table is to constrain the depth of the fingers in order to elaborate cavities and furrows of small sizes that allow reaching a great detail in the graphical representations of objects, people, and landscapes. In fact, some artists in Vanuatu and Africa have also used this technique to make drawings that require very long furrows, see fig. 2(c). Equations (1) and (2) suggest that the right performance of this inventive method ends at 3 times the diameter of the artist finger (or the object used to make craters and furrows): although furrows may grow at penetration depths above $z/d = 3$, craters do not. Furthermore, sand piles are used to increase details in a drawing. In general, during the deposition of grains through a narrow funnel, surface avalanches induce dispersion of grains. Our findings indicate that artists need to minimize the mass of the grains or the relative height $\zeta$, in order to reduce the size of the piles (see fig. 6). Very small piles (used by artists to create subtle details) need gentle deposition, where jamming is weakened by controlling the movement of the little finger of the hand.

There are still questions to be answered about the physics behind the creation of drawings in sand. Future work should explore how the size of cavities and furrows depends on the displacement velocity of the penetrating object and its geometry, grain shape, packing fraction, and even whether sand is dry or wet. Also, what the maximum size of the grains is to avoid jamming during the material deposition and what the minimum size is to avoid van der Waals forces are important questions.

## 4 Conclusions

We study the relations between three observables in sand drawing (the diameters of craters, furrows and piles) and some control parameters: the diameter of the penetrating bar, its penetration depth, the amount of piled grains, and the diameter of a deposition funnel. We found simple exponential and power laws that collapsed by length rescaling through the diameter of the bar (first two observables) and grain diameter (third observable). We show that there is the necessity to use shallow penetrations to make thinner (and therefore clearer) lines and cavities. This allows artists to produce complex drawings with more independent lines which are related to the power form of the curves. Indeed, even if interconnected traces do form graceful drawings, artists have the constriction of a limiting diameter of three times the size of the penetrating object used to make them (saturating exponential). On the other hand, we show that to form smaller piles it is required to use a small amount of grains deposited through a funnel with a small diameter.

Overall, we claim that granular physics has a coauthorship in artistic sand creations. Through simple exponential and power laws describing penetration and deposition, granular physics is able, indeed, to reveal the key elements of this art.

This work has been supported by CONACYT, Mexico, under grant 220962. We would like to express our gratitude to artists D. Myriam, K. Simonova, A. Woinowa, J. Denevan, and A. Amador for permission to use some of their drawings.

## Author contribution statement

JG-G carried out all the experiments and performed the analysis of the data. JG-G and JCR-S contributed in the discussion of the results and preparation of the manuscript. JCR-S supervised the research.

## References

1. L.P. Hurlburt, Rev. Bellas Art. **25**, 26 (1976).
2. Lord Rayleigh, Proc. London Math. Soc. **14**, 170 (1883).
3. G.I. Taylor, Proc. R. Soc. London A **201**, 192 (1950).
4. E.M. de la Calleja, S. Zetina, R. Zenit, Phys. Fluids **26**, 091102 (2014).
5. S. Zetina, F.A. Godinez, R. Zenit, PLoS ONE **10**, e0126135 (2015).
6. A. Herczyński, C. Cernuschi, L. Mahadevan, Phys. Today **64**, 31 (2011) issue No. 6.
7. P.K. Haff, J. Fluid Mech. **134**, 401 (1983).
8. R. Rioboo, C. Bauthier, J. Conti, M. Voue, J. De Coninck, Exp. Fluids **35**, 648 (2003).
9. L. Xu, W.W. Zhang, S.R. Nagel, Phys. Rev. Lett. **94**, 184505 (2005).
10. A.L. Yarin, Annu. Rev. Fluid Mech. **38**, 159 (2006).
11. S.T. Thoroddsen, K. Takehara, Phys. Fluids **12**, 1265 (2000).
12. K. Simonova, available at `http://simonova.tv/`; D. Myriam, available at `http://tramage.com/`; A. Woinowa, available at `http://www.artsand.net/`; accessed 06-07-2015.
13. A. Amador, available at `http://www.andresamadorarts.com/`; J. Denevan, available at `http://www.jimdenevan.com/`; accessed 06-07-2015.
14. M. Ascher, Hist. Math. **15**, 201 (1988).
15. M. Ascher, *Ethnomathematics: A Multicultural View of Mathematical Ideas* (Brooks/Cole, Pacific Grove, 1990).
16. J. Green, *Drawn from the Ground: Sound, Sign and Inscription in Central Australian Sand Stories* (Cambridge University Press, Padstow, 2014).

17. D. Chavey, Cult. Sci. **21**, 191 (2010).
18. P. Gerdes, *Drawings from Angola: Living Mathematics* (Lulu.com, 2007).
19. G. Siromoney, R. Siromoney, K. Krithivasan, Comput. Graph. Image Process. **1**, 284 (1972).
20. T. Robinson, Forma **22**, 55 (2007).
21. R. Soller, S.A. Koehler, EPL **80**, 14004 (2007).
22. M.B. Stone, R. Barry, D.P. Bernstein, M.D. Pelc, Y.K. Tsui, P. Schiffer, Phys. Rev. E **70**, 041301 (2004).
23. V.K. Horvath, I.M. Janosi, P.J. Vella, Phys. Rev. E **54**, 2005 (1996).
24. E. Kolb, P. Cixous, N. Gaudouen, T. Darnige, Phys. Rev. E **87**, 032207 (2013).
25. J. Geng, E. Longhi, R.P. Behringer, D.W. Howell, Phys. Rev. E **64**, 060301 (2001).
26. L. Vanel, D. Howell, D. Clark, R.P. Behringer, E. Clement, Phys. Rev. E **60**, R5040 (1999).
27. J. Ai, J.Y. Ooi, J.F. Chen, J.M. Rotter, Z. Zhong, Mech. Mater **66**, 160 (2013).
28. R. Albert, M.A. Pfeifer, A.L. Barabasi, P. Schiffer, Phys. Rev. Lett. **82**, 205 (1999).
29. M.B. Stone, D.P. Bernstein, R. Barry, M.D. Pelc, Y.K. Tsui, P. Schiffer, Nature **427**, 503 (2004).
30. M.B. Stone, R. Barry, D.P. Bernstein, M.D. Pelc, Y.K. Tsui, P. Schiffer, Phys. Rev. E **70**, 041301 (2004).
31. M. Schröter, S. Nägle, C. Radin, H.L. Swinney, EPL **78**, 44004 (2007).
32. Z. Peng, X. Xu, K. Lu, M. Hou, Phys. Rev. E **80**, 021301 (2009).
33. A.W. Roberts, C.M. Wensrich, Chem. Eng. Sci. **57**, 295 (2002).
34. V.D. Nguyen, C. Cogné, M. Guessasma, E. Bellenger, J. Fortin, Appl. Therm. Eng. **29**, 1846 (2009).
35. G. Nick, P.B. Umbanhowar, D.I. Goldman, Phys. Rev. Lett. **105**, 12 (2010).